

RESEARCH

Open Access



Improved primary stability and load transfer of a customized osseointegrated transfemoral prosthesis compared to a commercial one

Giulia Galteri¹, Valentina Betti¹, Domenico Alesi², Stefano Zaffagnini², Marco Palanca¹, Emanuele Gruppioni³ and Luca Cristofolini^{1*}

Abstract

Background Transfemoral osseointegrated prostheses, like other uncemented prostheses experience the risk of aseptic loosening and post-operative periprosthetic fractures, with an incidence between 3% and 30%. To date, however, osseointegrated off-the-shelf prostheses are manufactured in a limited number of sizes, and some patients do not meet the strict eligibility criteria of commercial devices. A customized osseointegrated stem was developed and a pre-clinical in vitro investigation of the stem was performed, to evaluate its biomechanical performance.

Materials and methods Six human cadaveric femurs were implanted with commercial stems, while the six contralateral were implanted with customized stems. Three more femurs that did not meet the eligibility criteria for the commercial stems were implanted with the customized stems. Two different loading scenarios (compression-flexion, and torsion) were simulated to measure the primary implant stability and the load transfer. For both loading scenarios, the displacements of the implant with respect to the host bone, and the strains on the bone surface were measured using digital image correlation (DIC). To measure the pull-out force, a tensile force was applied to the prostheses.

Results The translational inducible micromotions during the compression-flexion test of the OsteoCustom stem were more than 4 times smaller than the commercial one ($p < 0.05$). The rotational inducible micromotions of the OsteoCustom stem were more than 3 times smaller than the commercial one ($p < 0.05$). Similar results were found from the torsional test. The full-field strain distribution of the commercial stem showed a slightly higher strain concentration near the stem tip (maximum principal strain = $1928 \pm 127 \mu\epsilon$) than the OsteoCustom (maximum principal strain = $1758 \pm 130 \mu\epsilon$). Similar results were found for the femurs that did not meet the eligibility criteria for the commercial stems and could be implanted with the OsteoCustom. No statistically significant difference was found in the extraction force between the two groups.

Discussion and conclusion These results support the hypothesis that the OsteoCustom stem can offer better primary stability and load distribution compared to commercial implants. The outcome highlighted the potential

[†]Giulia Galteri and Valentina Betti share the first Authorship.

*Correspondence:
Luca Cristofolini
luca.cristofolini@unibo.it

Full list of author information is available at the end of the article



© The Author(s) 2025. **Open Access** This article is licensed under a Creative Commons Attribution-NonCommercial-NoDerivatives 4.0 International License, which permits any non-commercial use, sharing, distribution and reproduction in any medium or format, as long as you give appropriate credit to the original author(s) and the source, provide a link to the Creative Commons licence, and indicate if you modified the licensed material. You do not have permission under this licence to share adapted material derived from this article or parts of it. The images or other third party material in this article are included in the article's Creative Commons licence, unless indicated otherwise in a credit line to the material. If material is not included in the article's Creative Commons licence and your intended use is not permitted by statutory regulation or exceeds the permitted use, you will need to obtain permission directly from the copyright holder. To view a copy of this licence, visit <http://creativecommons.org/licenses/by-nc-nd/4.0/>.

benefits of the OsteoCustom prosthesis, which is capable of including a wider range of femoral anatomies than the current standard.

Keywords Lower-limb amputation, Transfemoral osseointegrated prosthesis, *In vitro* biomechanical test, Primary stability, Stem-bone load transfer, Implant micromotions

Introduction

In European countries, 15 to 30 out of every 100,000 subjects undergo a lower limb amputation every year [1], and this number is expected to increase [2]. The use of osseointegrated prostheses in the treatment of transfemoral amputation as an alternative solution to socket prostheses reported several advantages [3–5]. However, osseointegrated prostheses, like other uncemented prostheses experience the risk of aseptic loosening and post-operative periprosthetic fractures with an incidence between 3% and 30% [6–9]. Bone resorption induced by stress-shielding at the osteotomy level (distal part of the femur) [10] is a frequent and potentially catastrophic scenario. Indeed, (i) adverse bone resorption increases the risk of periprosthetic bone fractures, (ii) it can be expected to compromise the implant stability and (iii) it reduces the bone stock available in case a revision surgery is needed [11, 12]. Moreover, an inadequate contact area between the prosthesis and the bone after the implantation could lead to excessive post-operative relative motions and to aseptic loosening. To reduce the risk of implant instability, and to maintain physiological load transfer from the implant to the bone, surgeons aim to achieve as much contact area as possible, especially near the osteotomy level [13–15].

To date, however, osseointegrated off-the-shelf prostheses are manufactured in a limited number of sizes, where only the diameter and length of the implant vary, thus failing to consider the variability of the other anatomical parameters of the medullary canal [16]. Consequently, some patients do not meet the strict eligibility criteria of commercial osseointegrated prostheses. For instance, osseointegrated implantation is not advisable for patients whose bone diameter does not fall within a specified range (e.g., excessively small/large medullary canal) or in cases where canal reaming would result in excessively thin cortical bone remaining around the implant [16].

In order to increase the number of patients that can be treated with osseointegrated prostheses, the prosthesis design should follow the anatomical variability of the femoral medullary canal. Indeed, it has been demonstrated that there is significant inter-subject anatomical variability in parameters like diameter, radius of curvature, conicity, and ellipticity of the canal [17]. Thus, a new concept of osseointegrated transfemoral prosthesis has been developed [16]. In that study, it has been shown that the fit-and-fill can be improved if the stem matches the

diameter, radius of curvature, conicity, and ellipticity of the host femur. Indeed, from a database of 70 CT images (in which 19 did not meet the eligibility criteria for commercial stem implantation), it was found that a customized stem (later referred to as “OsteoCustom”) would significantly reduce the amount of bone to be removed if compared to one of the most common commercial stems. Similarly, the stem-bone contact area was also greater for a OsteoCustom stem, particularly at the distal resection level [16]. However, while improving fit-and-fill is generally expected to provide better implant stability and better load transfer, this claimed advantage has to be proven. Therefore, to perform the pre-clinical investigation of the OsteoCustom device, it is extremely important to evaluate its biomechanical performance, in particular its implant primary stability and load transfer, which are crucial for the success of uncemented prostheses.

This paper aims to assess whether the OsteoCustom stem could be a reliable alternative to an osseointegrated commercial press-fit stem. In particular, we hypothesized that the OsteoCustom stem, if compared to a commercial stem would provide (i) better primary stability under a combination of compression and flexion load, and torsional load, and in terms of pull-out extraction force (ii) similar or better load transfer in terms of strain distribution in the host bone. Moreover, we hypothesized that femurs failing to satisfy the eligibility criteria for standard commercial stems could be successfully implanted with the OsteoCustom stem and achieve similarly good primary stability.

Materials and methods

Design of the study

To assess the implant stability, load transfer, and whether the OsteoCustom stem would allow the inclusion of more cases, the specimens were categorized into two groups:

- **Group A:** femurs that did meet the eligibility criteria for the commercial stem (and thus were implanted with both the commercial and the OsteoCustom stems). In particular, six human cadaveric femurs (49 ± 11 years old, Table 1) were implanted with a commercial stem OFI-C (Badal-X, OTN implants, Netherlands), while the six contralateral femurs were implanted with the OsteoCustom stem. Two of the femurs implanted with the OFI-C stem were the same that were tested in the previous methodological study [18].

Table 1 Details of the donors and of the implanted stems. GROUP A (top) contained paired femurs where one femur of each donor was implanted with the commercial stem, and the contralateral one with the OsteoCustom stem; GROUP B (bottom) consisted of femurs whose anatomy could not meet the eligibility criteria of the commercial stem and were implanted (unpaired) only with the OsteoCustom one. The right column reports the size of the stem. For the OFI-C the nominal diameter is indicated. For the OsteoCustom stems the size is indicated by five numbers: the first number indicates the diameter (in mm) of the proximal portion of the stem, the second and third numbers indicate the major and minor axes (in mm) of the elliptical distal section; the fourth number indicates the radius of curvature of the stem (in mm), the fourth number indicates the angle of internal/external rotation of the plane of curvature with respect to the major axis of the elliptical cross-section)

Group A								
Type of prosthesis	Donor ID	Side	Age (year)	Sex	BMI (kg/m ²)	Weight (kg)	Height (cm)	Prosthesis (size)
Commercial stem	#1 (*)	Left	58	M	34	100	170	15
	#2	Right	52	M	24	72	172	16
	#3	Right	56	M	35	113	180	16
	#4	Left	57	F	44	127	170	15
	#5 (*)	Right	44	F	21	54	163	15
	#6	Right	27	M	42	142	183	17
OsteoCustom stem	#1	Left	58	M	34	100	170	15-18-15-849-69
	#2	Right	52	M	24	72	172	16-19-16-664-33
	#3	Right	56	M	35	113	180	16-23-20-739-47
	#4	Right	57	F	44	127	170	15-18-15-632-17
	#5	Left	44	F	21	54	163	16-19-16-664-33
	#6	Left	27	M	42	142	183	16-23-20-944-17
Group B								
OsteoCustom stem	#7	Right	44	M	32	82	160	12-16-15-641-10
	#8	Left	59	M	33	109	183	12-16-15-695-18
	#9	Left	58	F	32	81.6	160	13-19-15-683-3

Note (*): For the commercial stem, the Specimens from donors 1, and 5, were previously tested as part of the study where the experimental protocol was developed and validated [18]

- **Group B:** femurs that did not meet the eligibility criteria for the commercial stem (and thus were not tested with the OFI-C), were implanted with the OsteoCustom stem. This group included 3 unpaired femurs (51 ± 8 years old, Table 1).

Two different relevant loading scenarios were simulated to measure the implant stability and the load transfer: a combination of flexion and compression, and torsion. For both the loading scenarios, the displacements of the implant with respect to the host bone and the surface strains were measured throughout the test using a digital image correlation (DIC) system.

Ethics approval

The study complied with the Declaration of Helsinki and was approved by the Ethical Committee of the University of Bologna (reference n. 113063, 10th May 2021). The human cadaveric femurs were obtained through an ethically approved international donation program (Anatomy Gift Registry, USA).

Specimen preparation

To avoid alteration of the mechanical properties, the specimens were kept hydrated and stored at -28 °C.

Each specimen was scanned with computed tomography (CT, VCT LightSpeed, GE medical systems, USA, slice thickness = 0.6 mm, in-plane resolution = 0.5 mm) to determine the anatomy of the bone and the dimension of the femoral canal. The soft tissues were carefully removed using surgical tools, the femurs were aligned and their proximal end was embedded in an aluminum pot, following a validated procedure described in [18].

Prosthetic implants

Based on the CT scans, two surgeons experienced in transfemoral amputation and osseointegrated implantation identified the optimal size for the commercial stem, and validated the design of the OsteoCustom stem (see also below). The femurs were osteotomized at a typical level for this kind of implant (between 150 and 200 mm from the condyles). The same osteotomy level was applied to both femurs from the same pair.

Replicas of the Badal X stem (OTN Implants) were generated with reverse engineering, and 3D printed (Lincotek, Italy) with direct metal laser sintering (DMLS) technology from Ti6Al4V (Fig. 1left). To implant the prostheses, flexible reamers were first used, followed by replicas of the proprietary Badal X rasps of increasing

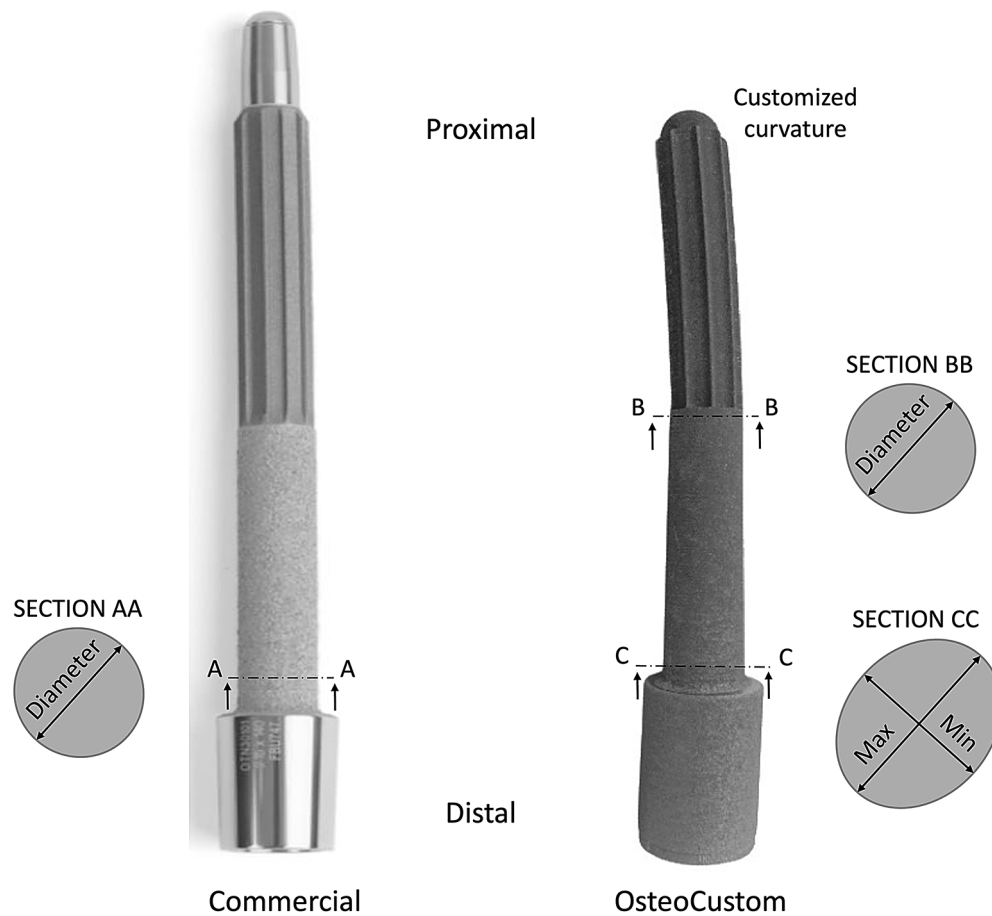


Fig. 1 LEFT: Replica of the commercial stem OFI-C, RIGHT: Example of the OsteoCustom stem. Also indicated are the main dimensions and the most relevant cross-sections. For the Commercial stem, the only relevant dimension was the diameter (Section A), which is constant along the stem. For the OsteoCustom stem, the parameters customized to each femur were: the diameter of the section at mid-length (Section B, which is circular), and the major (Max) and minor (Min) axes of the most distal section (Section C, which was elliptical), and the radius of curvature of the proximal portion

size. Finally, the commercial stems were press-fitted into the bone using a hammer as per clinical practice.

The OsteoCustom stems were monolithic and were shaped as follows (Fig. 1 right):

- A proximal portion, with customized diameter and radius of curvature of the canal.
- A distal portion, with customized conicity, and ellipticity to fit the shape of the medullary canal. Moreover, the intra-extra rotation angle between the planes of curvature of the proximal portion was also customized.

The anatomical parameters were defined as follows:

- Diameter of the proximal portion: each cross-section was analyzed by fitting a circumference, thus estimating the corresponding diameters. The diameter of the proximal part of the stem was calculated as the average diameter of the medullary canal in the relevant proximal cross-sections.

- Conicity of the distal portion: the conicity in the distal part of the stem was computed as the difference between the diameter of the most distal section and the minimum diameter within the analyzed segment (which often, but not always, corresponded to the diameter of the most proximal section).
- Ellipticity of the distal portion: the ellipticity of the distal part of the stem was defined as the difference between the major and the minor axes in the most distal section of the medullary canal.
- Curvature of the proximal portion: each cross-section was further best fitted as an ellipse, identifying its centroid and estimating the major and minor axes. The curvature of the canal was determined by reconstructing the arc of a circle best fitting the centroids along the entire length of the stem.
- Angle of internal/external rotation: From the distal cross-section, the angle was defined as the angle of

the plane of curvature with respect to the major axis of the elliptical cross-section).

More details about the design of the OsteoCustom stem are reported in [16]. To implant the OsteoCustom stem, the medullary canals were first reamed with flexible reamers up to the designed diameter. The distal part of the canal was then prepared with rasps having dedicated diameter, conicity, and ellipticity. Then, the OsteoCustom stems were press-fitted into the bone using a hammer as per clinical practice. Both the commercial and the OsteoCustom implanted stems were CT scanned (VCT LightSpeed, GE medical systems, USA, slice thickness = 0.6 mm, in-plane resolution = 0.5 mm) (Fig. 2).

All the stem sizes implanted are reported in Table 1.

Biomechanical cyclic tests to assess the primary stability (implant micromotions)

To evaluate the primary stability, two relevant and critical loading scenarios were simulated:

- A combination of compression and flexion load emulating the peak load during gait, corresponding to heel strike (the largest moment occurs on the mediolateral axis and ranges between 20 and 40 Nm [19]) [18];
- A pure torsional load emulating one of the possible loosening mechanisms for nearly straight stems.

A uniaxial-servo-hydraulic testing machine (8500 Instron, UK) equipped with a 10 kN load cell was used. In order to test the first relevant condition (compression-flexion), the specimens were tilted by 10° in flexion and 10° in adduction and were constrained proximally, while the force was applied distally [18]. To avoid transmission

of any undesired component of load, free horizontal translations were granted using low-friction linear bearings (Fig. 3A). A preload of 150 N was applied. Then, each specimen was loaded by applying 100 sinusoidal cycles at 1 Hz between 150 N and 850 N. This resulted in a combination of compression and a peak bending moment of 30 Nm at the osteotomy level.

The pure torsional test was performed with a protocol adapted from the previous one. A multiaxial testing machine (Mod. MAS2-S, MIB4.0, Bologna, Italy) with a 6-components load cell (HBK, Darmstadt, Germany, 150 Nm full-scale) was used. The specimens were constrained proximally, and the load was applied distally. A preload of 2 Nm was applied. Then, a pure torsional load of 10 Nm was applied for 100 cycles at 0.5 Hz (Fig. 3B).

To measure the relative motion between the prosthesis and the host bone a 3D digital image correlation system (Aramis Adjustable 12 M, GOM, Braunschweig, Germany) equipped with four cameras (12 MegaPixels 4096 × 3000 pixels, 8 bit) was used. The surface of the femur was prepared with a random speckle pattern while a set of fiducial markers were placed on the distal extremity of the prosthesis. The DIC tracked the motion in both of areas with the speckle pattern and the fiducial markers. The spatial micromotions of the prosthesis with respect to the host bone were analyzed as the displacements (three components of translation and three components of rotations) between the prosthesis (tracked through the set of fiducial markers attached) and the distal extremity of the femur (tracked through the surface speckle pattern) throughout the test (Fig. 3C).

To quantify the systematic and random errors affecting the DIC-measured displacements, a zero-displacement analysis was performed using a known configuration similar to [20]. The permanent migrations were computed as the difference between the position of the stem inside the bone at the last and at the first load peak. The inducible micromotions were computed as the difference between the position of the stem inside the bone at the load peak and valley of each cycle throughout the test. More technical details can be found in the supplementary materials and in [18].

Measurement of the load transfer (strain on bone surface)

As bone remodeling is mainly driven by cyclic loads [12, 21], this part of the study focused on the loading condition that most frequently occurs in the femur, i.e. gait. Thus, the simulated heel strike phase of gait described above was also used to investigate the load transfer to the femur, following a method previously developed and validated [18]. In this case, the DIC system was used to measure the strains on the bone surface. To quantify the systematic and random errors affecting the

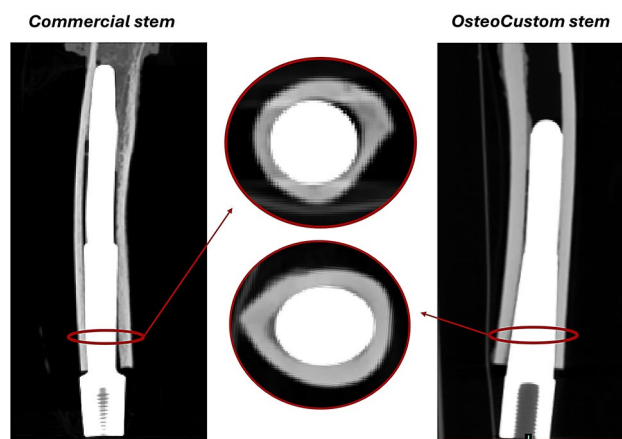


Fig. 2 LEFT) CT scan of a typical implantation of the commercial stem (sagittal plane, with a zoom of a distal cross-section showing the contact area of the prosthesis into the bone). RIGHT) CT scan of the contralateral implantation of the OsteoCustom stem (sagittal plane, with a zoom on a distal cross-section)

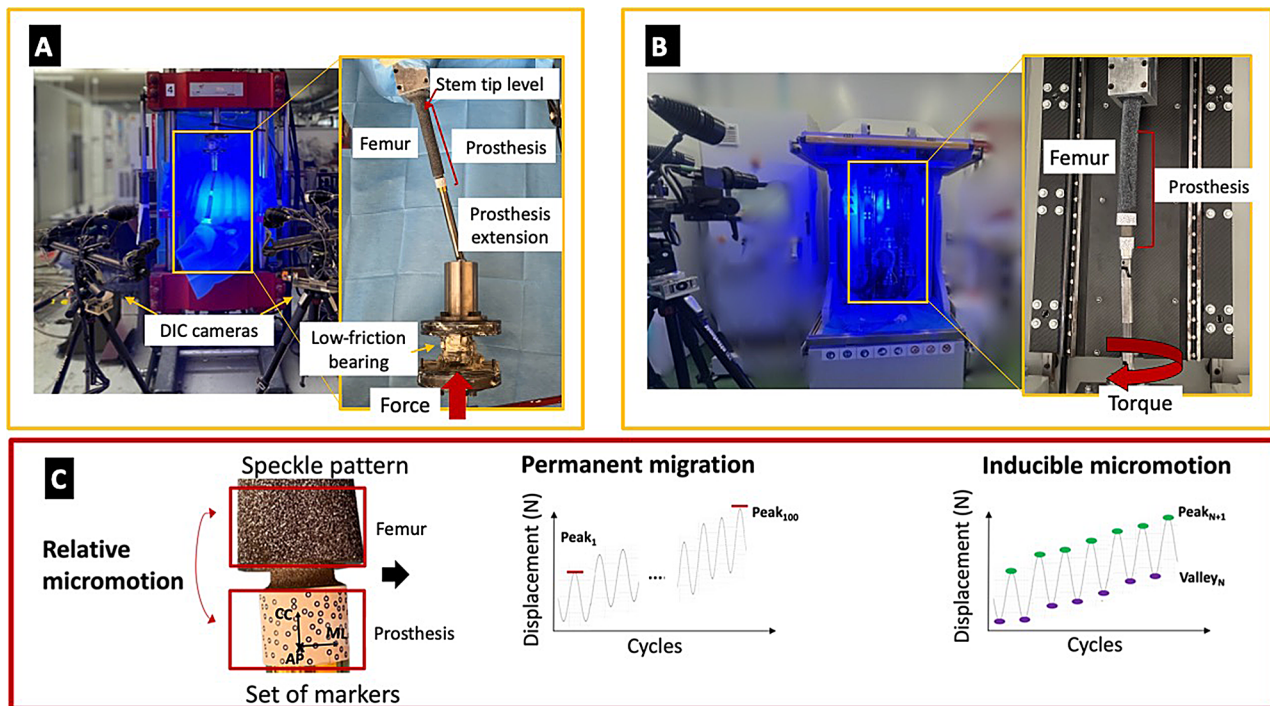


Fig. 3 **A**) Overview of the experimental setup of the compression-flexion test: a uniaxial-servo-hydraulic testing machine was used to deliver the force to the distal end of the specimens. The four cameras of the DIC framed the implanted specimen from a mediolateral and anterior view. **B**) Overview of the experimental setup for the torsional cyclic test. The four cameras of the DIC framed the medial, posterior, and lateral sides of the implanted specimen. **C**) Schematic of the analysis of the DIC-measured displacements to compute the permanent migrations and the inducible micromotions. The frames corresponding to the load peaks and load valleys were extracted. The permanent migrations were computed as the difference between the position of the implant relative to the bone at the last peak and at the first peak (Peak₁₀₀–Peak₁). The inducible micromotions were computed as the difference between the position of the implant relative to the bone at each load peak and at the corresponding valley (Peak_N–Valley_N). A subsection of **(C)** is reproduced from [18] under the Creative Commons Attribution License (CC BY)

DIC-measured strains, a zero-strain analysis was performed using a known configuration similar to [20].

As an indicator of load transfer, the full-field distribution of the maximum (ϵ_1) and minimum (ϵ_2) principal strains at the peak load on the surface of the femur was measured. A qualitative analysis of the entire surface was performed first. The quantitative investigation of the maximum and minimum principal strains focused on two regions of interest (ROIs):

- ROI 1, proximal, was centered on the stem tip and covered the femur from 10 mm proximal to 10 mm distal to the stem tip;
- ROI 2, distal, covered the femur by 20 mm proximal from the osteotomy.

More details can be found in the supplementary materials and in [18].

Pull-out test

To measure the pull-out force, a tensile force was applied to the prosthesis after completing the mechanical test (both compression-flexion and torsional tests).

A uniaxial-servo-hydraulic testing machine (8500 Instron, UK) was used to apply the load. The femurs were clamped proximally (ensuring axial alignment). To ensure that a pure axial force was applied, the prostheses were attached to the actuator of the testing machine through a spherical joint. The specimens were loaded in displacement control with a constant rate of 5 mm/min, similar to [22]. The force and displacement were recorded with a frequency of 25 Hz throughout the test.

Statistical analysis

The data of the permanent migrations, inducible micromotion, maximum and minimum principal strain were reported as the median and interquartile range (IQR).

In order to test the hypothesis that the OsteoCustom stem provides better primary stability and load transfer compared to the commercial stems, and to evaluate if the OsteoCustom stem of group B achieved similar primary stability as the OsteoCustom stem of group A, the following statistical analyses were performed (Prism 9.5.1, GraphPad Software, USA) with the level of significance set to 0.05.

The primary stability (permanent migrations, inducible micromotions, and pull-out extraction force) and the load transfer (maximum and minimum principal strain distribution on the ROIs) measured on the OsteoCustom specimens were compared with the ones measured on the commercial specimens with a non-parametric Wilcoxon paired test (data were not normal and homoscedastic, Shapiro-Wilk test and Levene's test). A non-parametric Mann-Whitney test was used to assess the difference of primary stability and load transfer between the OsteoCustom femurs of group A and the OsteoCustom femurs of group B.

Results

DIC-measured implant primary stability (implant micromotion)

The systematic error affecting the DIC-measured implant micromotions was less than 1 micrometer for the translation and less than 0.05° for the rotations. The random error was less than 15 micrometers for the translation and less than 0.05° for the rotations.

For group A (containing the pairs of femurs where both the commercial and the OsteoCustom stems were implanted) for the compression-flexion test, the translational permanent migrations of the OsteoCustom stem were significantly lower than the commercial one in the anteroposterior (AP: $p=0.016$) and craniocaudal (CC: $p=0.032$) directions (Fig. 4). The difference along the mediolateral direction were not significant (ML: $p=0.078$). The rotational permanent migrations of the commercial and the OsteoCustom stems were similar in all directions (AP: $p=0.5$; CC: $p=0.29$; ML: $p=0.28$). The translational inducible micromotions through the compression-flexion test of the OsteoCustom stem were significantly lower than the commercial one in all directions (AP: $p=0.015$; CC: $p=0.016$; ML: $p=0.031$). The rotational inducible micromotions of the OsteoCustom stem were significantly lower compared to the commercial one in all directions (AP: $p=0.015$; CC: $p=0.031$; ML: $p=0.032$).

Regarding the torsional test of group A, the permanent migrations and the inducible micromotion of the translational permanent migrations of the OsteoCustom stem were significantly lower than the commercial one along the mediolateral axis (ML: $p=0.047$), but not along the anteroposterior (AP: $p=0.42$) and craniocaudal (CC: $p=0.42$) directions (Fig. 5). The rotational permanent migrations were similar for the commercial and the OsteoCustom stems in all directions (AP: $p=0.36$; CC: $p=0.25$; ML: $p=0.12$). The translational inducible micromotions through the torsional test of the OsteoCustom stem were significantly lower than the commercial one along the anteroposterior (AP: $p=0.015$) and the mediolateral (ML: $p=0.016$) axes, but not along the

craniocaudal one (CC: $p=0.15$). The rotational inducible micromotions of the OsteoCustom stem were significantly lower than the commercial one around the craniocaudal axis (i.e. around the axis of application of the torque, CC: $p=0.015$) while the other two components of rotation were not significantly different, and comparable to the measurement uncertainty of the DIC.

Additionally, group B (femurs not eligible for implantation with the commercial stem but only with OsteoCustom) was compared against the femurs of Group A implanted with the OsteoCustom stem. For both the combination of compression and flexion, and the torsional tests, there was no significant difference between Group A and B for the permanent migrations and inducible micromotions in terms of translation and rotations ($p>0.12$).

DIC-measured load transfer (strain on bone surface)

The systematic error affecting the DIC-measured strains on the bone surface was less than 17 microstrains, while the random error was less than 25 microstrains, in line with previous DIC analyses [18, 25]. The full-field strain maps for the two prostheses were qualitatively similar (Fig. 6).

In particular, the commercial stem induced a slightly higher strain concentration near the stem tip (ROI 1) than the OsteoCustom: the maximum principal strain (ϵ_1) on ROI 1 for the commercial stem was $1928 \mu\epsilon$ (median, IQR = $127 \mu\epsilon$ between 6 specimens), while for the OsteoCustom stems was $1758 \mu\epsilon$ (median, IQR = $130 \mu\epsilon$) (Fig. 7). This difference was not statistically significant ($p=0.078$). The minimum principal strains in ROI 1 showed smaller values, and no significant differences ($p=0.42$).

Near the resection level (ROI 2) no statistically significant difference was observed between the commercial and the OsteoCustom stems both for the maximum (ϵ_1 , $p=0.34$) and for the minimum principal strain (ϵ_2 , $p=0.42$).

Additionally, group B (femurs not eligible for implantation with the commercial stem but only with OsteoCustom) was compared against the femurs of Group A implanted with the OsteoCustom stem. For both the combination of compression and flexion, and the torsional tests, there was no significant difference between Groups A and B for the maximum principal strain (ϵ_1 , $p>0.20$) and minimum principal strain (ϵ_2 , $p>0.15$) on the ROIs.

Pull-out extraction force

No statistically significant difference was found in the extraction force ($p=0.43$) of the commercial stems (median = 2400 N, IQR = 800 N) and OsteoCustom stems of group A (median = 2707 N, IQR = 900 N)

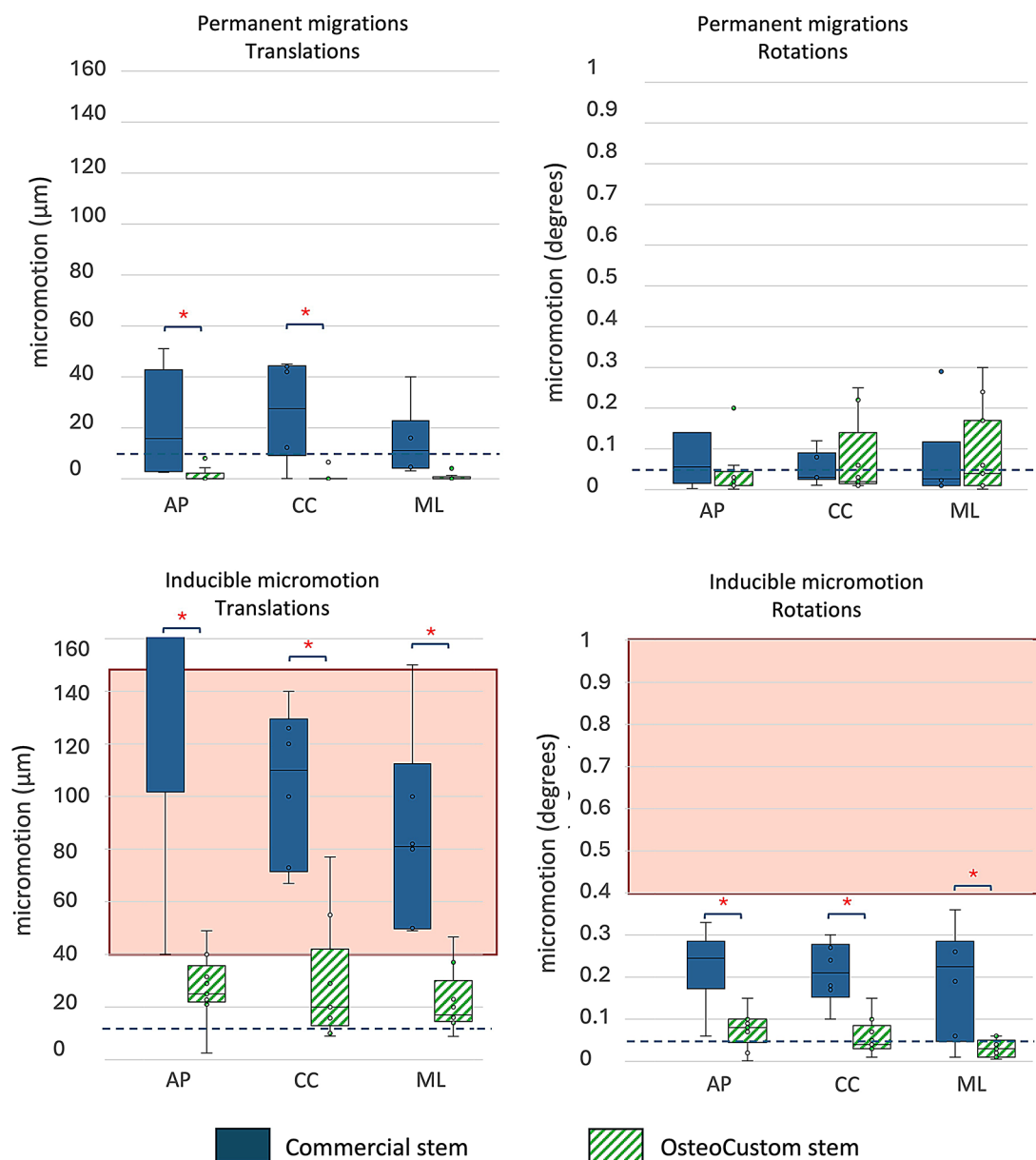


Fig. 4 Translational and rotational primary stability in the compression-flexion test in terms of permanent migrations and inducible micromotions around the craniocaudal (CC), anteroposterior (AP), and mediolateral (ML) axes for both the commercial and the OsteoCustom stems. For each group, the individual specimens (small circles), the median (horizontal line), the 25–75% percentile (solid box), and the 5th and 95th percentile (whiskers) are indicated. Statistically significant differences ($p < 0.05$) between the commercial and the customized stem are highlighted with *. For the inducible micromotions, the pink band indicates the critical range of micromotions which is likely to prevent osseointegration [23, 24]. Therefore, the inducible micromotions of a stable implant should be lower than the pink bands. The dotted line represents the intrinsic error affecting the DIC-measured micromotion

(Fig. 8). Moreover, the OsteoCustom stems of group B showed a comparable extraction force (median = 1785 N, IQR = 1000 N) compared to the OsteoCustom stems of group A.

Discussion

Osseointegrated prostheses for lower limb amputees are exposed to the risk of adverse bone remodeling and aseptic loosening ([9, 26, 27]). Moreover, osseointegrated

off-the-shelf prostheses are manufactured in a limited number of sizes, thus failing to cover the variability of the other anatomical parameters of the medullary canal [16]. Consequently, several patients do not meet the strict eligibility criteria for commercial osseointegrated prostheses.

In this study, an osseointegrated customized press-fit stem (OsteoCustom) and a commercial one (OFI-C) were implanted in human cadaveric femurs, to assess whether

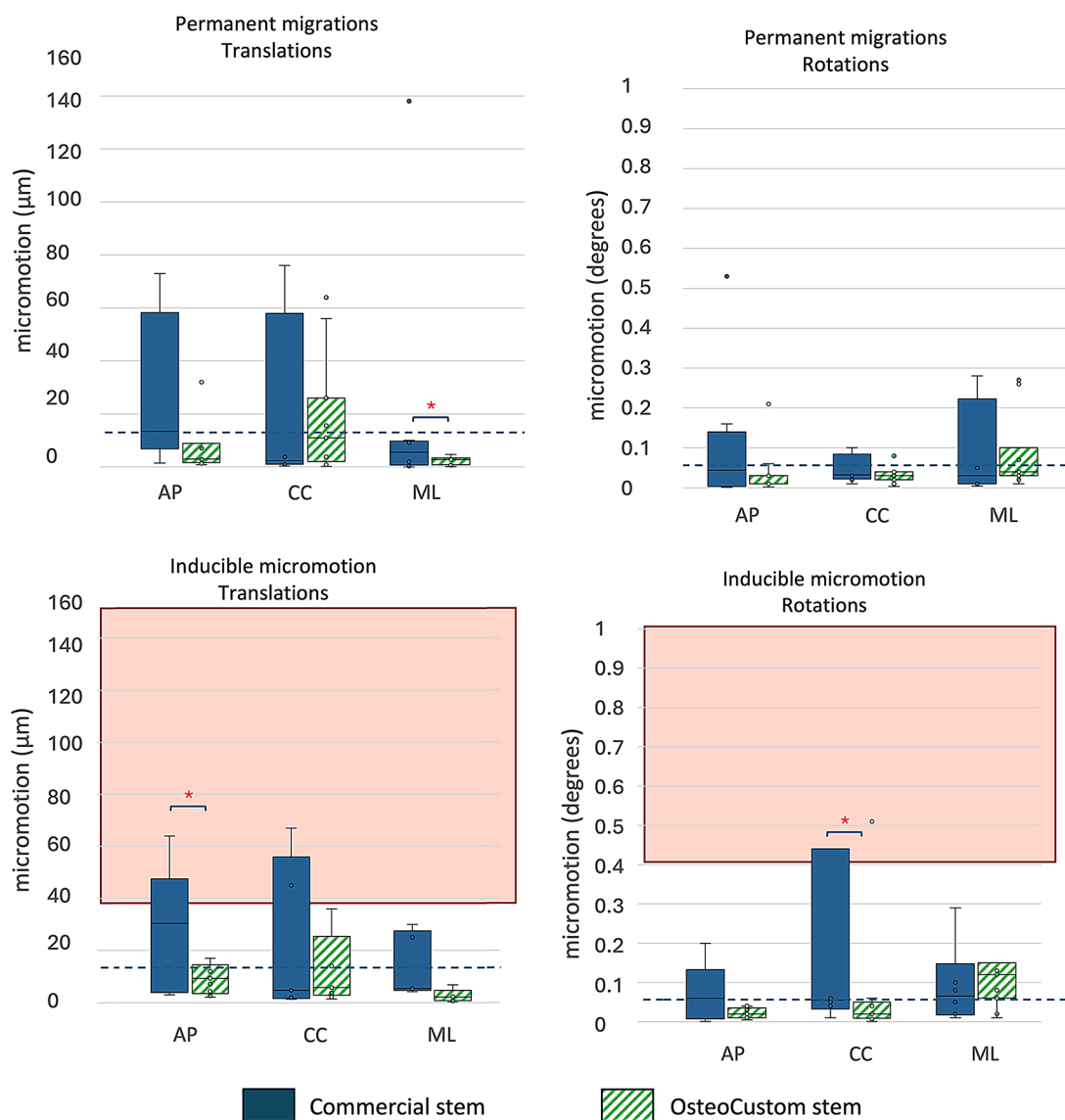


Fig. 5 Translational and rotational primary stability through the torsional test in terms of permanent migrations and inducible micromotions around the craniocaudal (CC), anteroposterior (AP), and mediolateral (ML) axes for both the commercial and the OsteoCustom stems. For each group, the individual specimens (small circles), the median (horizontal line), the 25–75% percentile (solid box), and the 5th and 95th percentile (whiskers) are indicated. Statistically significant differences ($p < 0.05$) between the commercial and the customized stem are highlighted with *. For the inducible micromotions, the pink band indicates the critical range of micromotions which is likely to prevent osseointegration [23, 24]. Therefore, the inducible micromotions of a stable implant should be lower than the pink bands. The dotted line represents the intrinsic error affecting the DIC-measured micromotion

the OsteoCustom stem could be an advantageous alternative to the commercial ones, particularly in case of femurs that do not meet the eligibility criteria of the commercial stem. The implants were tested under different relevant loading scenarios, to assess if the OsteoCustom would achieve a better implant primary stability and load transfer than the commercial one.

In terms of micromotions, smaller permanent translations were measured for the OsteoCustom stem, compared to the commercial stem, during both the compression-flexion and torsional tests. Conversely, permanent rotations were similar for the two stems. The

inducible micromotions during the compression-flexion were smaller for the OsteoCustom stem compared to the commercial stem across all directions. In particular, the translational inducible micromotions through the compression-flexion test of the OsteoCustom stem were more than 4.5 times smaller than the commercial one in all directions ($p < 0.05$) and below the critical threshold. The rotational inducible micromotions of the OsteoCustom stem were more than 3 times smaller than the commercial one in all directions ($p < 0.05$). Similar results were found for the torsional tests. Indeed, under torsional loading the translational inducible micromotions through

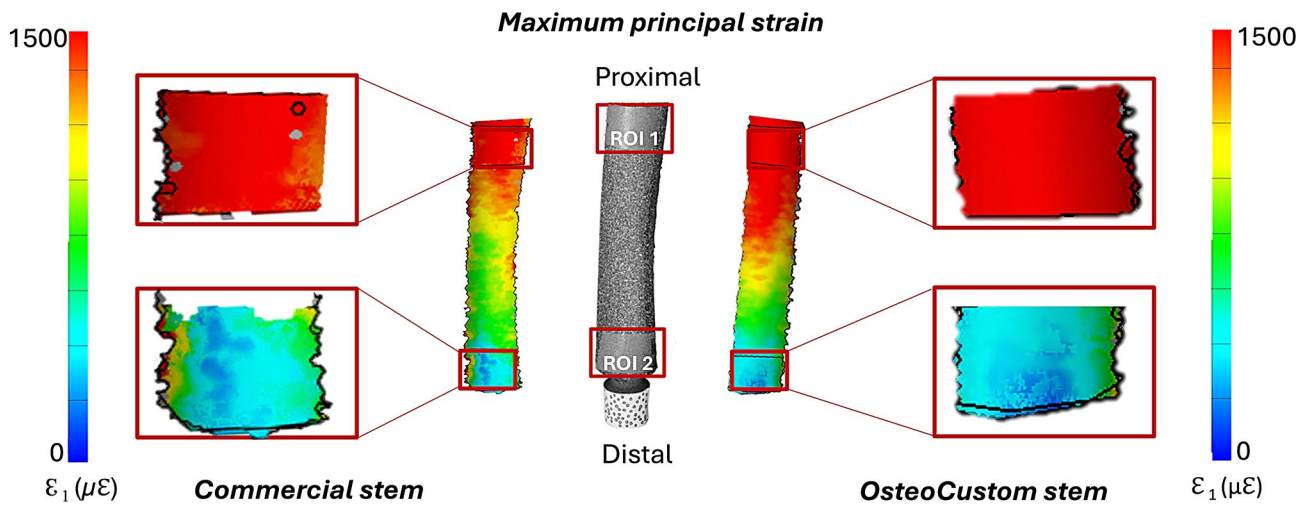


Fig. 6 Full-field distribution of the maximum principal strains (ϵ_1) of one typical specimen with commercial stem (left) and the contralateral with OsteoCustom stem (right) at the peak load (simulating the heel strike phase of gait)

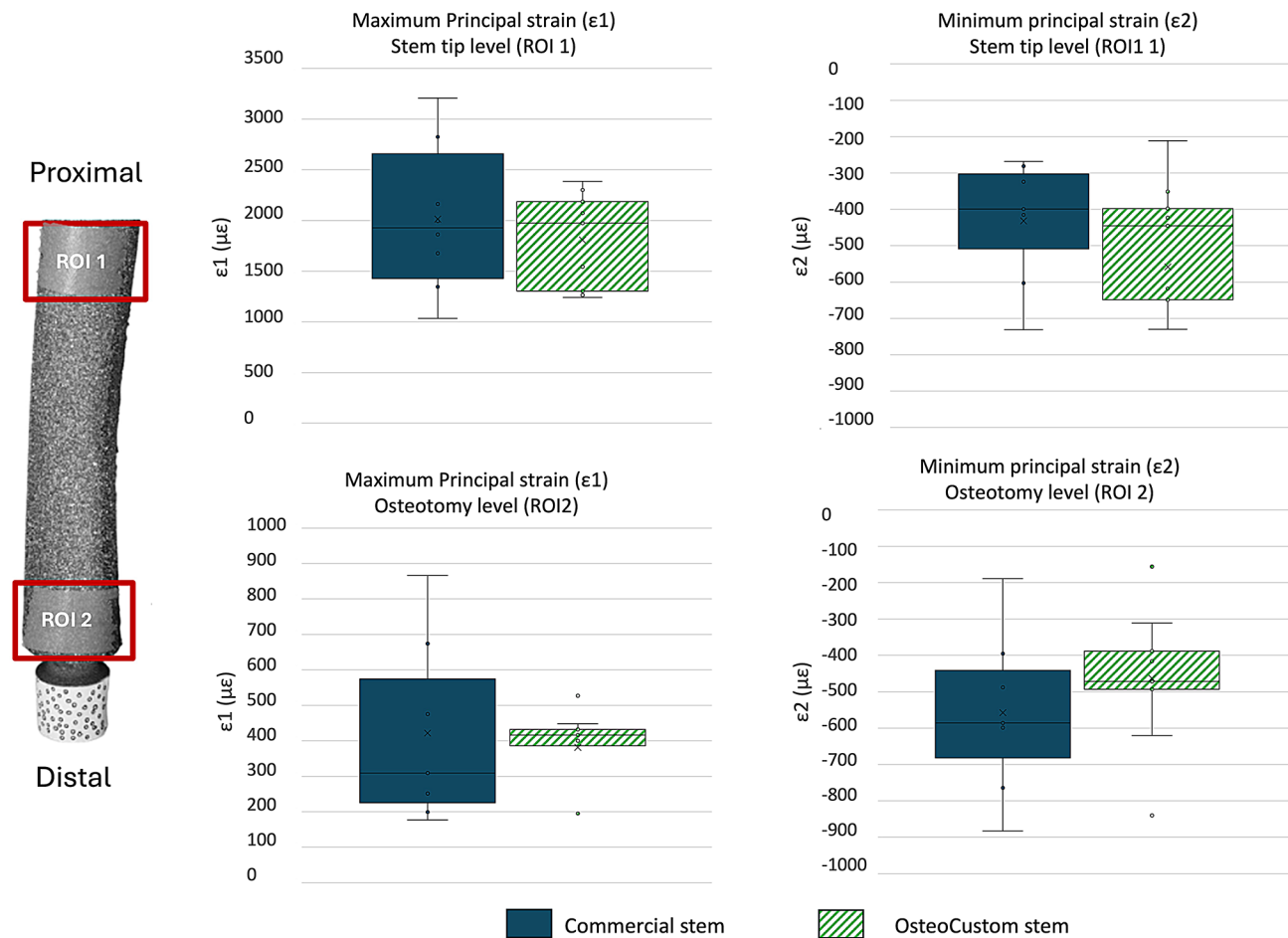


Fig. 7 Comparison of the strain distribution in ROI 1 (top charts) and ROI 2 (bottom). The maximum principal strain (ϵ_1 , charts on the left) and minimum principal strain (ϵ_2 , on the right) were analyzed for the commercial and the contralateral OsteoCustom implants. For each group, the individual specimens (small circles), the median (horizontal line), the 25–75% percentile (solid box), and the 5th and 95th percentile (whiskers) are indicated. No statistically significant differences were found between the commercial and the customized stem ($p > 0.05$)

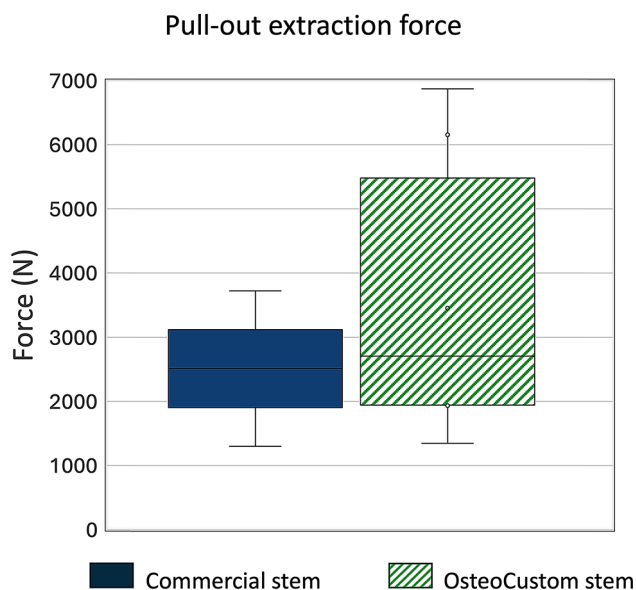


Fig. 8 Comparison of the pull-out force of the commercial stems and OsteoCustom stems. For each group, the median (horizontal line), the 25–75% percentile (solid box), and the 5th and 95th percentile (whiskers) are indicated. No statistically significant differences were found between the commercial and the customized stem ($p > 0.05$)

the compression-flexion test of the OsteoCustom stem were more than 2 times smaller than the commercial one, but in this case the difference was statistically significant only on the anteroposterior axis ($p < 0.05$). The rotational inducible micromotions of the OsteoCustom stem were smaller than the commercial one, and in this case the difference was statistically significant on the craniocaudal axis ($p < 0.05$).

This is critical since excessive inducible micromotions (40–150 micrometers [23, 24]) can lead to aseptic loosening and complications. Indeed, the early implant migration and the correct load transfer from the prosthesis to the bone are strong predictors for future aseptic loosening, and crucial for the long-term success of the osseointegrated implants [22, 27]. Few studies can be found in the literature where micromotions of osseointegrated transfemoral implants were measured. Barnes reported inducible micromotions below of 20 micrometers when testing a simplified geometry of a femoral stem [22]. For comparison, inducible micromotions of the order of 30 micrometers were measured for uncemented hip stems when tested in vitro [21]. The present results highlight the efficacy of the OsteoCustom in providing a stable primary mechanical stability. Indeed, the customization of the stem grants a better fit-and-fill of the stem into the bone [16]. Moreover, the OsteoCustom stem provides an option for those anatomies that would not meet the criteria for commercial implants. Indeed, three OsteoCustom stems were successfully implanted in femurs that would not be suitable for the commercial stem (group B),

and showed similar permanent migrations and inducible micromotions compared to the OsteoCustom stems of group A and below the critical thresholds. This outcome confirms the advantage for all femur anatomies of taking into account the anatomical parameters (e.g. conicity, ellipticity) of the intramedullary canal [16, 17].

The DIC analysis of strains revealed differences in strain profiles near the stem tips, although these were not statistically significant. The OsteoCustom stem exhibited reduced strain concentration compared to the commercial stem, which could translate into decreased susceptibility to bone fractures or stress. The magnitude of the maximum principal strains measured on the bone surface near the stem tip was within the physiological range for the cortical bone, and decreased towards the distal region (close to the osteotomy) [28]. Similarly to [29], reduced strains were observed in the distal region for both the commercial and the customized stems. This is an undesirable condition as it can trigger adverse bone remodeling. The difference between the commercial and the customized stem was not statistically significant in this respect. Moreover, the strain distributions are comparable to those reported in in vitro studies using strain gauges on selected points [29–31]. Furthermore, the strain maps of the femurs of group B showed qualitative similarities with group A, suggesting that the OsteoCustom may serve as a viable alternative for femurs that did not meet the eligibility criteria of commercial stems.

The pull-out force of the OsteoCustom was slightly higher than the commercial stem, but there was no statistical significance. The pullout force found for the OsteoCustom was comparable to the results for other prototype stems [22, 32]. Also, the OsteoCustom groups A and B showed comparable extraction force, confirming how customization could widen the indications, without compromising the primary mechanical stability.

For some of the parameters, a remarkable inter-specimen variability was observed. This is likely due to a combination of differences between donors and surgical variability. In clinical practice, the “outliers” are those patients experiencing an implant failure (this is hopefully a small number, falling in the tails of the statistical distribution). These are indeed the cases that require the most attention. Similarly, in our biomechanical tests, we chose not to exclude the “outliers” as they are likely representative of the fraction of possible patients at risk of failure.

For the commercial stem three different sizes were used, which were chosen as the most ideal size for the respective femur to be implanted. No specific correlation was found between the results and the implant size. Indeed, due to the limited sample size, a detailed analysis of the correlation between stem size and micromotions would have limited statistical power.

The main limitation of this study relates to the fact that the proposed method can only simulate the early post-operative period, as it is not possible to simulate bone ingrowth and remodeling on ex vivo specimens. For this reason, the mid-term and long-term changes (including osseointegration and bone remodeling) cannot be taken into account. This is indeed common to all similar in vitro studies ([22, 29]). However, this information is a valuable indicator of the primary stability, which is crucial for the short-term and long-term success of uncemented prostheses [33]. In fact, implant micromotions and an incorrect load transfer in the early post-operative period can interfere with the process of osseointegration and affect the long-term stability. In addition, the test specimens did not include donors older than 65 years, since aging generally leads to a deterioration in bone quality [34]. However, this is not a limitation with respect to prostheses for amputees, as in most of the clinical studies, the patients are younger than 60 years [15, 35].

Another limitation relates to the commercially available stem (OFI-C, Badal X) chosen as a benchmark in the present study. Other commercial designs include press-fit stems, such as the one tested in this study (e.g., OPL), but also threaded implants (e.g., OPRA). For this comparison, the stem selected was the one exhibiting the most similar geometry to the OsteoCustom.

Surgical implantation was unavoidably affected by some variability. To avoid unrealistic variability, all the implants were performed by experienced surgeons, who followed the standard procedure for preparing the medullary canals and press-fitting the implants, using the dedicated surgical instrumentation. To mitigate the possible consequences of the variability, the femurs within each pair were osteotomized at the same level.

The pull-out test does not represent a common failure scenario for femoral osseointegrated stems. However, the pull-out test is used when a fast and reproducible test is needed and is often used to test other prosthetic devices (in some cases it is prescribed by the FDA [36]). Therefore, we included it in our study for completeness and to allow comparisons with other published studies.

The procedure for designing and manufacturing customized stems can be expected to be more expensive than standardized ones. A detailed cost-benefit analysis for a customized stem would be outside the goal of the present study and is not currently available, but it will be necessary and important to perform it before making decisions about clinical use of customized stems.

Conclusions

This study supports the hypothesis that the OsteoCustom stem can offer better primary stability and load distribution compared to commercial implants. The outcome highlighted the potential benefits of the OsteoCustom

prosthesis, which is capable of including a wider range of femoral anatomies than the current standard. In particular, the customization of the stem offered a better matching with the anatomical variability of the femurs, possibly providing a reliable solution for patients who did not meet the eligibility criteria for the commercial stem.

Supplementary Information

The online version contains supplementary material available at <https://doi.org/10.1186/s13018-025-05476-x>.

Supplementary Material 1

Acknowledgements

The Authors wish to thank Sara Montanari, Giulia Cavazzoni, and Margherita Pasini for their help with the test sessions, and Francesco Vai and Roberto Budini for their technical support.

Author contributions

GG: conceptualization, methodology, investigation, resources, formal analysis, data curation, writing original draft, review, and editing. VB: conceptualization, writing original draft, review and editing. MP: conceptualization, supervision, methodology, review, and editing. DA: investigation, review and editing. SZ: investigation, review and editing. EG: project administration, funding acquisition, supervision, review and editing. LC: conceptualization, methodology, review and editing, project administration, funding acquisition, supervision. Giulia Galteri and Valentina Betti share the 1st Authorship. All authors contributed to the article and approved the submitted version.

Funding

This study was partly funded by INAIL (PR19-CR-P5-OsteoCustom).

Data availability

No datasets were generated or analysed during the current study.

Declarations

Ethical approval

The study complied with the Declaration of Helsinki and was approved by the Ethical Committee of the University of Bologna (reference n. 113063, 10th May 2021). The human cadaveric femurs were obtained through an ethically approved international donation program (Anatomy Gift Registry, USA).

Competing interests

The authors declare no competing interests.

Author details

¹Department of Industrial Engineering, Alma Mater Studiorum-University of Bologna, Bologna, Italy

²IRCCS Istituto Ortopedico Rizzoli, Bologna, Italy

³Centro Protesi INAIL, Vigorso di Budrio, Bologna, Italy

Received: 11 October 2024 / Accepted: 8 January 2025

Published online: 27 January 2025

References

1. Hughes W, Goodall R, Saliccioli JD, Marshall DC, Davies AH, Shalhoub J. Editor's Choice – Trends in Lower Extremity Amputation Incidence in European Union 15 + Countries 1990–2017. *Eur. J. Vasc. Endovasc. Surg.*, vol. 60, no. 4, pp. 602–612, Oct. 2020. <https://doi.org/10.1016/j.ejvs.2020.05.037>
2. Ziegler-Graham K, MacKenzie EJ, Ephraim PL, Travison TG, Brookmeyer R. Estimating the Prevalence of Limb Loss in the United States: 2005 to 2050. *Arch. Phys. Med. Rehabil.*, vol. 89, no. 3, pp. 422–429, Mar. 2008. <https://doi.org/10.1016/j.apmr.2007.11.005>

3. Gerzina C, Potter E, Haleem AM, Dabash S. The future of the amputees with osseointegration: a systematic review of literature. *J Clin Orthop Trauma*. Feb. 2019;11:S142–8. <https://doi.org/10.1016/j.jcot.2019.05.025>.
4. Örgel M et al. Dec., Comparison of functional outcome and patient satisfaction between patients with socket prosthesis and patients treated with transcutaneous osseointegrated prosthetic systems (TOPS) after transfemoral amputation. *Eur. J. Trauma Emerg. Surg.*, vol. 48, no. 6, pp. 4867–4876, 2022, <https://doi.org/10.1007/s00068-022-02018-6>
5. Hebert JS, Rehani M, Stiegelmar R. Osseointegration for Lower-Limb amputation: a systematic review of clinical outcomes. *JBJS Rev*. Oct. 2017;5(10):e10–10. <https://doi.org/10.2106/JBJS.RVW.17.00037>.
6. Ranker A, Örgel M, Beck JP, Krettek C, Aschoff HH. Transkutane osseointegrierte Prothesensysteme (TOPS) zur Versorgung Oberschenkelamputierter: Eine sechsjährige retrospektive Analyse des aktuellen Prothesendesigns in Deutschland. *Rehabil.*, vol. 59, no. 06, pp. 357–365, Dec. 2020, <https://doi.org/10.1055/a-1223-3205>
7. Reetz D, Atallah R, Mohamed J, van de Meent H, Frölke JPM, Leijendekkers R. Safety and Performance of Bone-Anchored Prostheses in Persons with a Transfemoral Amputation: A 5-Year Follow-up Study. *J. Bone Jt. Surg.*, vol. 102, no. 15, pp. 1329–1335, Aug. 2020, <https://doi.org/10.2106/JBJS.19.01169>
8. Leijendekkers RA, van Hinte G, Frölke JP, van de Meent H, Nijhuis-van der MWG, Sanden, Staal JB. Comparison of bone-anchored prostheses and socket prostheses for patients with a lower extremity amputation: a systematic review. *Disabil Rehabil*. May 2017;39(11):1045–58. <https://doi.org/10.1080/09638288.2016.1186752>.
9. Galteri G, Cristofolini L. In vitro and in silico methods for the biomechanical assessment of osseointegrated transfemoral prostheses: a systematic review. *Front Bioeng Biotechnol*. 2023. <https://doi.org/10.3389/fbioe.2023.1237919>.
10. Xu W, Robinson K. X-ray image review of the bone remodeling around an osseointegrated trans-femoral implant and a finite element simulation case study. *Ann. Biomed. Eng.*, vol. 36, no. 3, pp. 435–443, Mar. 2008, <https://doi.org/10.1007/s10439-007-9430-7>
11. Burchard R, Graw JA, Soost C, Schmitt J. Stress shielding effect after total hip arthroplasty varies between combinations of stem design and stiffness—a comparing biomechanical finite element analysis. *Int Orthop*. Aug. 2023;47(8):1981–7. <https://doi.org/10.1007/s00264-023-05825-7>.
12. Cristofolini L. A critical Analysis of stress shielding evaluation of Hip Prostheses, 1997.
13. Kang N et al. Jun., Radiological evaluation before and after treatment with an osseointegrated bone-anchor following major limb amputation—a guide for radiologists. *Skeletal Radiol.*, vol. 53, no. 6, pp. 1033–1043, 2024, <https://doi.org/10.1007/s00256-023-04524-z>
14. Schwarze M, Hurschler C, Seehaus F, Correa T, Welke B. Influence of transfemoral amputation length on resulting loads at the osseointegrated prosthesis fixation during walking and falling. *Clin. Biomech. Bristol Avon*, vol. 29, no. 3, pp. 272–276, Mar. 2014, <https://doi.org/10.1016/j.clinbiomech.2013.11.023>
15. Khemka A, FarajAllah CI, Lord SJ, Bosley B, Muderis MA. Osseointegrated total hip replacement connected to a lower limb prosthesis: a proof-of-concept study with three cases. *J Orthop Surg*. Jan. 2016;11:13. <https://doi.org/10.1186/s13018-016-0348-3>.
16. Betti V, et al. Advantages of customization of osseointegrated implants in transfemoral amputees: a comparative analysis of surgical planning. *J Orthop Surg*. Aug. 2024;19(1):520. <https://doi.org/10.1186/s13018-024-04944-0>.
17. Betti V, Aldieri A, Cristofolini L. A statistical shape analysis for the assessment of the main geometrical features of the distal femoral medullary canal. *Front. Bioeng. Biotechnol.*, vol. 12, Apr. 2024, <https://doi.org/10.3389/fbioe.2024.1250095>
18. Galteri G et al. Mar., Reliable in vitro method for the evaluation of the primary stability and load transfer of transfemoral prostheses for osseointegrated implantation. *Front. Bioeng. Biotechnol.*, vol. 12, 2024, <https://doi.org/10.3389/fbioe.2024.1360208>
19. Frossard L, Laux S, Geada M, Heym PP, Lechler K. Load applied on osseointegrated implant by transfemoral bone-anchored prostheses fitted with state-of-the-art prosthetic components. *Clin Biomech*. Oct. 2021;89:105457. <https://doi.org/10.1016/j.clinbiomech.2021.105457>.
20. Palanca M, Brugo TM, Cristofolini L. Use of digital image correlation to investigate the biomechanics of the vertebra. *J. Mech. Med. Biol.*, vol. 15, no. 02, p. 1540004, Apr. 2015. <https://doi.org/10.1142/S0219519415400047>
21. Cristofolini L, Teutonico AS, Savigni P, Erani P, Viceconti M. Preclinical assessment of the long-term endurance of cemented hip stems. Part 1: Effect of daily activities - a comparison of two load histories. *Proc. Inst. Mech. Eng. [H]*, vol. 221, no. 6, pp. 569–584, Jun. 2007, <https://doi.org/10.1243/09544119JHEM183>
22. Barnes SC, Clasper JC, Bull AMJ, Jeffers JRT. Micromotion and Push-Out Evaluation of an Additive Manufactured Implant for Above-the-Knee Amputees. *J. Orthop. Res.*, vol. 37, no. 10, pp. 2104–2111, Oct. 2019, <https://doi.org/10.1002/jor.24389>
23. Pilliar RM, Lee JM, Maniopoulos C. Observations on the effect of movement on bone ingrowth into porous-surfaced implants. *Clin. Orthop.*, no. 208, pp. 108–113, Jul. 1986.
24. Engh CA, Bobyn JD, Glassman AH. Porous-coated hip replacement. The factors governing bone ingrowth, stress shielding, and clinical results. *J Bone Joint Surg Br. Jan.* 1987;69(1):45–55. <https://doi.org/10.1302/0301-620X.69B1.3818732>.
25. Palanca M, et al. The strain distribution in the lumbar anterior longitudinal ligament is affected by the loading condition and bony features: an in vitro full-field analysis. *PLoS ONE*. 2020;15(1):e0227210. <https://doi.org/10.1371/journal.pone.0227210>.
26. Al Muderis M, Khemka A, Lord SJ, Van de Meent H, Frölke JPM. Safety of Osseointegrated Implants for Transfemoral Amputees: A Two-Center Prospective Cohort Study. *J. Bone Jt. Surg.*, vol. 98, no. 11, pp. 900–909, Jun. 2016, <https://doi.org/10.2106/JBJS.15.00808>
27. Juhnke D-L, Beck JP, Jeyapalina S, Aschoff HH. Fifteen years of experience with Integral-Leg-Prosthesis: Cohort study of artificial limb attachment system. *J Rehabil Res Dev*. 2015;52(4):407–20. <https://doi.org/10.1682/JRRD.2014.11.0280>.
28. Lanyon IE. Bone Remodeling, Mechanical Stress, and Osteoporosis. *HF Luca Ed Osteoporos. Univ. Park Press Baltim.* 1980 Pp 129–138, 1980.
29. Tomaszewski PK, Lasnier B, Hannink G, Verkerke GJ, Verdonchot N. Experimental assessment of a new direct fixation implant for artificial limbs. *J Mech Behav Biomed Mater*. May 2013;21:77–85. <https://doi.org/10.1016/j.jmbm.2013.02.012>.
30. Cristofolini B, Toni. In vitro testing of a novel limb salvage prosthesis for the distal femur. *Clin. Biomech.*, vol. 13, no. 8, pp. 608–615, Dec. 1998, [https://doi.org/10.1016/S0268-0033\(98\)00024-2](https://doi.org/10.1016/S0268-0033(98)00024-2)
31. Ahmed K, et al. Experimental validation of an ITAP Numerical Model and the Effect of Implant Stem stiffness on bone strain energy. *Ann Biomed Eng. Apr.* 2020;48(4):1382–95. <https://doi.org/10.1007/s10439-020-02456-6>.
32. Welke B, Hurschler C, Föllner M, Schwarze M, Calliess T. Stiffness and ultimate load of osseointegrated prosthesis fixations in the upper and lower extremity. *Biomed Eng OnLine*. 2013;12(1):70. <https://doi.org/10.1186/1475-925X-12-70>.
33. ten Brinke B, Hesselink B, Eygendaal D, Hoelen MA, Mathijssen NMC. Early fixation of the humeral component in stemless total shoulder arthroplasty: a radiostereometric and clinical study with 24-month follow-up. *Bone Jt J. Jan.* 2022;104–B:76–82. <https://doi.org/10.1302/0301-620X.104B1.BJJ-2021-0945.R1>.
34. Glismann K, Konow T, Lampe F, Ondruschka B, Huber G, Morlock MM. Small design modifications can improve the primary stability of a fully coated tapered wedge hip stem. *PLoS ONE*. Apr. 2024;19(4):e0300956. <https://doi.org/10.1371/journal.pone.0300956>.
35. Hagberg K, Ghassemi Jahani S-A, Kulbacka-Ortiz K, Thomsen P, Malchau H, Reinholdt C. A 15-year follow-up of transfemoral amputees with bone-anchored transcutaneous prostheses: mechanical complications and patient-reported outcomes. *Bone Jt J. Jan.* 2020;102–B:55–63. <https://doi.org/10.1302/0301-620X.102B1.BJJ-2019-0611.R1>.
36. U.S. Department of Health and Human Services, Food and Drug Administration, Center for Devices and Radiological Health, Orthopedic Devices Branch, Division of General, Restorative, and Neurological Devices, and Office of Device Evaluation. *Knee Joint Patellofemoral and Femorotibial Metal/Polymer Porous-Coated Uncemented Prostheses - Class II Special Controls Guidance Document for Industry and FDA*. Jan. 16, 2003.

Publisher's note

Springer Nature remains neutral with regard to jurisdictional claims in published maps and institutional affiliations.